THE JOURNAL OF BIOLOGICAL CHEMISTRY VOL. 283, NO. 8, pp. 4912–4920, February 22, 2008


# Heparin Strongly Enhances the Formation of $\beta_2$-Microglobulin Amyloid Fibrils in the Presence of Type I Collagen*

Received for publication, March 29, 2007, and in revised form, November 27, 2007 Published, JBC Papers in Press, December 3, 2007, DOI 10.1074/jbc.M702712200

**Annalisa Relini[‡§], Silvia De Stefano[‡], Silvia Torrassa[‡], Ornella Cavalleri[‡§], Ranieri Rolandi[‡§], Alessandra Gliozzi[‡§], Sofia Giorgetti[¶‖], Sara Raimondi[¶], Loredana Marchese[¶], Laura Verga[‖], Antonio Rossi[¶], Monica Stoppini[‖**], and Vittorio Bellotti[¶‖**1]**

*From the [‡]Department of Physics, University of Genoa, [§]Consorzio Nazionale Interuniversitario per le Scienze Fisiche della Materia (CNISM), I-16146 Genoa, Italy, [¶]Department of Biochemistry, University of Pavia, [‖]Laboratori di Biotecnologie IRCCS Policlinico San Matteo, I-27100 Pavia, Italy, and **Consorzio Interuniversitario Istituto Nazionale Biostrutture e Biosistemi, (INBB), I-00136 Roma, Italy*

**The tissue specificity of fibrillar deposition in dialysis-related amyloidosis is most likely associated with the peculiar interaction of $\beta_2$-microglobulin ($\beta_2$-m) with collagen fibers. However, other co-factors such as glycosaminoglycans might facilitate amyloid formation. In this study we have investigated the role of heparin in the process of collagen-driven amyloidogenesis. In fact, heparin is a well known positive effector of fibrillogenesis, and the elucidation of its potential effect in this type of amyloidosis is particularly relevant because heparin is regularly given to patients subject to hemodialysis to prevent blood clotting. We have monitored by atomic force microscopy the formation of $\beta_2$-m amyloid fibrils in the presence of collagen fibers, and we have discovered that heparin strongly accelerates amyloid deposition. The mechanism of this effect is still largely unexplained. Using dynamic light scattering, we have found that heparin promotes $\beta_2$-m aggregation in solution at pH 6.4. Morphology and structure of fibrils obtained in the presence of collagen and heparin are highly similar to those of natural fibrils. The fibril surface topology, investigated by limited proteolysis, suggests that the general assembly of amyloid fibrils grown under these conditions and *in vitro* at low pH is similar. The exposure of these fibrils to trypsin generates a cleavage at the C-terminal of lysine 6 and creates the 7–99 truncated form of $\beta_2$-m ($\Delta$N6$\beta_2$-m) that is a ubiquitous constituent of the natural $\beta_2$-m fibrils. The formation of this $\beta_2$-m species, which has a strong propensity to aggregate, might play an important role in the acceleration of local amyloid deposition.**

Dialysis-related amyloidosis (DRA),[2] a severe disease arising as a complication of long term hemodialysis, involves the deposition of $\beta_2$-microglobulin ($\beta_2$-m) amyloid fibrils in bones and ligaments. $\beta_2$-m constitutes the light chain of the major histocompatibility complex class I and CD1 (1), and in normal catabolism, it is continuously released in the serum and cleared from the circulation by the kidney. The replacement of renal function by hemodialysis does not efficiently remove $\beta_2$-m. The persistent increase of its plasma concentration is associated with $\beta_2$-m deposition in the osteotendineous system, which is the specific target tissue of this type of amyloidosis. Among extra-cerebral amyloidoses, DRA represents the most striking case of tissue-specific targeting. Although other organs can be involved, bones and ligaments never escape amyloid deposition. Homma (2) first pointed out that collagen might be involved in determining this tissue specificity and demonstrated a collagen/$\beta_2$-m interaction.

We have recently determined the binding properties governing the collagen/$\beta_2$-m interaction, and we found that the latter is quite weak but is enhanced when $\beta_2$-m is truncated at the N-terminal end, and the pH is reduced from 7.4 to 6.4 (3). We subsequently demonstrated that fibrillar collagen (type I), which is abundant in skeletal tissues, is a potent promoter of $\beta_2$-m fibrillation at 37 °C and pH 6.4 (4); we chose this pH because it was compatible with pathophysiological conditions including the presence of inflammatory processes frequently associated with this amyloid deposition. Incubation of $\beta_2$-m in the presence of fibrillar collagen yielded amyloid fibrils, the morphology of which was similar to that of *ex vivo* fibrils extracted from the amyloid deposits of patients affected by DRA. We hypothesized that the positively charged patches distributed over the collagen surface could promote an increase of $\beta_2$-m concentration in the solvent surrounding the collagen fiber and also the proper orientation of $\beta_2$-m that facilitates an ordered polymerization (4). Type I collagen must assume its highly ordered fiber conformation, typical of bones and ligaments, to promote amyloid formation and deposition. When microfibrils alignment is more disordered, as in the skin (5), collagen, although very abundant in this district, does not represent a good inducer of amyloid fibril deposition. In fact, cuta-

* This work was supported in part by Italian Ministry of Education, University and Research Grants (PRIN 2005053998, 2005061114, and 2006058958; FIRB RBNE03PX83), the University of Genoa (Progetti di Ateneo), Fondazione CARIGE, Fondazione Cariplo (progetto Nobel), European Union grant EURAMY, Regione Lombardia, and Ricerca Finalizzata (Ministero della Salute). The costs of publication of this article were defrayed in part by the payment of page charges. This article must therefore be hereby marked "*advertisement*" in accordance with 18 U.S.C. Section 1734 solely to indicate this fact.

[1] To whom correspondence should be addressed: Dipartimento di Biochimica, Università di Pavia, via Taramelli, 3b-27100 Pavia, Italy. Tel.: 39-0382-987932; Fax: 39-0382-423108; E-mail: vbellot@unipv.it.

[2] The abbreviations used are: DRA, dialysis-related amyloidosis; $\beta_2$-m, $\beta_2$-microglobulin; $\Delta$N6$\beta_2$-m, form of $\beta_2$-m lacking the first six N-terminal residues; GAG, glycosaminoglycan; DRA, dialysis-related amyloidosis; AFM, atomic force microscopy; MALDI-TOF, matrix-assisted laser desorption ionization time-of-flight.

neous amyloidosis is rare in DRA, although a few cases have been reported (6).

Glycosaminoglycans (GAGs) are a constitutive component (7) of amyloid deposits, including those associated with DRA. *In vitro* studies have shown that GAGs enhance the nucleation of amyloid-$\beta$ peptides (8) and favor fibril formation and stabilization (9). Heparin and at a lesser extent heparan sulfate are reported to significantly increase the rate of fibrillation of $\alpha$-synuclein (10) and gelsolin (11). Extensive experimental evidence show that among GAGs, heparin is particularly effective in accelerating both the fibril formation (11) and extension (12), and it has been proposed that such behavior is highly dependent on the sulfate groups present in this GAG (11). However, the molecular mechanisms involved in the enhancement of aggregation by heparin and other GAGs are still unknown. Furthermore, *in vivo* studies have demonstrated the coincident deposition of amyloidogenic protein and GAGs (13), and in a mouse model of amyloid protein A (AA) amyloidosis a resistance against the amyloid deposition can be achieved through the overexpression of heparanase, which degrades heparan sulfate (14). A key role of GAGs in causing the amyloid deposition is also proved by the effectiveness of therapeutic agents able to displace GAGs from the amyloid fibrils (15).

The investigation of the effects of heparin on the fibrillation of $\beta_2$-m is particularly relevant because heparin is commonly used as an anticoagulant in the therapeutic treatment of patients affected by DRA (16). Heparin has been reported to inhibit the depolymerization of $\beta_2$-m fibrils *in vitro* (17) and to promote the extension of preformed fibril seeds, both in the presence (12) and in the absence (18), of trifluoroethanol. Finally, the exposure of heparin to $\Delta$N6$\beta_2$-m, which is an ubiquitous constituent of the natural $\beta_2$-m fibrils, allows the formation of amyloid fibrils even in physiologic buffer (19).

In this study we have tested the effect of the co-presence of collagen and heparin on the fibrillogenesis of full-length $\beta_2$-m. We have mainly used atomic force microscopy to investigate the sample morphology and limited proteolysis to study the conformation of $\beta_2$-m in the fibrils obtained in the presence of heparin. We performed light scattering measurements to test the effect of heparin on the aggregation process of $\beta_2$-m. Overall, our data indicate that the enhancing effect of heparin on amyloidogenesis is associated with an increased oligomerization of $\beta_2$-m.

## EXPERIMENTAL PROCEDURES

*Expression and Purification of Recombinant $\beta_2$-m*—$\beta_2$-m was produced as recombinant protein according to the procedure reported previously (20). The concentration of the protein solution was determined spectrophotometrically at 280 nm by using an extinction coefficient ($A_{1\ cm}^{1\%}$) of 16.17.

*Preparation of Type I Fibrillar Collagen*—Type I collagen was purified from calf skin as described previously (3). The purity of the collagen was checked by SDS-PAGE, and the concentration of the collagen solutions was determined by the hydroxyproline assay according to Huszar *et al.* (21). Fibrillar collagen was prepared by solubilizing purified collagen in 5 mM acetic acid. The solution was diluted 1:1 with a phosphate buffer (0.001 M magnesium chloride, 0.272 M sodium chloride, 0.005 M potassium chloride, 0.003 M potassium dihydrogen phosphate, 0.016 disodium hydrogen phosphate) pH 7.5 and incubated at 37 °C for 30 min.

*Aggregation of $\beta_2$-m*—Lyophilized $\beta_2$-m was dissolved in 50 mM ammonium acetate, pH 7.4, at the concentration of 2 mg/ml and centrifuged at 16,500 $\times$ *g* for 1 h to remove large aggregates. The supernatant was collected and filtered with a 20-nm pore filter; the protein concentration was then determined using a Jasco V-530 spectrophotometer. Aggregation experiments were performed at protein concentrations in the 40–50 $\mu$M range for AFM (atomic force microscopy) experiments and 160–170 $\mu$M range for thioflavin T assay, after acidification of the protein solution to pH 6.4 by using an HCl solution at pH 2. The final ammonium acetate concentration was in the 12–30 mM range. 20 $\mu$g of fibrillar collagen were suspended in 50 mM ammonium acetate, pH 6.4 and were added to the protein solution. The sample was incubated at 37 °C in the presence of 20 $\mu$M heparin sodium salt, low molecular weight (4000–6000) from porcine intestinal mucosa (Sigma-Aldrich). Furthermore, the same experimental conditions were used for the aggregation experiments in the presence of 1 mg/ml of $\Delta$N6$\beta_2$-m.

*Thioflavin T Assay*—Quantification of amyloid fibril formation was performed with the method described by LeVine (22). Thioflavin T concentration was 5 $\mu$M, and the buffer used was 50 mM glycine, pH 8.5. Measurements were made using a LS50 PerkinElmer spectrofluorometer with excitation at 455 nm; emission was collected at 485 nm. Slits were set at 5 mm.

*Limited Proteolysis and MALDI-TOF Experiments*—The aggregate constituted by fibrillar $\beta_2$-m grown on collagen in the presence of heparin was separated from the supernatant and washed twice with 50 mM ammonium bicarbonate. Comparative limited proteolysis experiments were performed on soluble $\beta_2$-m and fibrils obtained from $\beta_2$-m at pH 4.0 (20) and at pH 6.4 in the presence of collagen and heparin. Experiments were carried out by incubating the samples with trypsin (Sigma-Aldrich) and endoprotease AspN (Roche). Enzymatic digestions were all performed in 50 mM ammonium bicarbonate (pH 7.5) at 37 °C using an enzyme-to-substrate ratio 1:100 (w/w). The extent of the reaction was monitored on a time course basis by sampling the incubation mixture at different time intervals.

Peptide mixtures were analyzed by MALDI-TOF mass spectrometry using a Micromass spectrometer (Waters) in linear mode. The sample was solubilized in 0.2% trifluoroacetic acid, and the protein solution was mixed 1:1 with a solution of $\alpha$-cyano-4-hydroxycinammic acid, 10 mg/ml in acetonitrile, 0.2% trifluoroacetic acid 7:3 (v:v), applied onto the metallic sample plate and air dried. Mass calibration was performed using a sample of $\beta_2$-m soluble standard.

*Atomic Force Microscopy*—Aggregation of $\beta_2$-m in the presence of collagen and heparin was performed as described above, but a lower heparin concentration was employed (from 2 to 9 $\mu$M). The protein concentration was in the range between 17 and 50 $\mu$M. In addition, four or five aliquots of fibrillar collagen (instead of one) were added to the protein solution to allow sampling at different times of the aggregation reaction. Details of sample preparation, including pre-sonication of collagen, are the same described previously for aggregation experiments in

the presence of collagen alone (4). For AFM inspection, each collagen aliquot was extracted from the protein solution, deposited onto freshly cleaved mica, gently washed with buffer, and dried under a nitrogen stream. AFM images were acquired in tapping mode using a Multimode Scanning Probe microscope (Digital Instruments-Veeco, Santa Barbara, California), equipped with a "E" scanning head (maximum scan size 10 $\mu$m), and driven by a Nanoscope IV controller. Single beam uncoated silicon cantilevers (type OMCL-AC160TS, Olympus, Tokyo, Japan) were used. The drive frequency was around 300 kHz; the scan rate was between 0.3 and 0.8 Hz. Vertical displacements were calibrated measuring the depth of grating notches (180 nm) and the half-unit cell steps (1 nm) obtained by treating freshly cleaved mica with hydrofluoric acid. The horizontal displacements of the piezoelectric tubes were calibrated using a 3-$\mu$m pitch diffraction grating.

*Dynamic Light Scattering*—Dynamic light scattering measurements were performed at 25 °C using a Zetasizer Nano ZS (Malvern Instruments). This instrument exploits backscatter detection (173 °C) together with non-invasive detection optics (NIBS technology) and yields size distributions obtained by the analysis of the correlation function using an algorithm based on CONTIN. The latter uses the following power approximation for the scattered intensity: $I(r) \sim r^6$, $r < 100$ nm; $I(r) \sim r^2$, $r \geq 100$ nm (23). However, due to the high polydispersity of our system, such analysis only provides a qualitative estimate of the size distributions. Therefore, we chose to base the analysis of dynamic light scattering data on the comparison of the autocorrelation functions in the absence and in the presence of heparin. Experiments were performed incubating $\beta_2$-m at 37 °C in ammonium acetate 50 mM, pH 6.4. A set of experiments was also performed under the same conditions, but at pH 7.4. The protein concentration was between 260 and 300 $\mu$M. We tested heparin concentrations of 2 and 0.6 $\mu$M. Before starting the experiment, the protein solution was filtered with a 20-nm pore filter, and the protein concentration was determined after filtration using a Jasco V-530 spectrophotometer. The pH stability of the sample was checked as a function of time; the measurements at pH 7.4 were done under nitrogen to avoid possible pH changes induced in the small sample volume by the presence of atmospheric $CO_2$.

*Cross-linkage of $\beta_2$-m Oligomers*—$\beta_2$-m at 100 $\mu$M in phosphate buffer (pH 7.8) was incubated with 200 $\mu$M disuccinimidyl glutarate, used as a cross-linker (freshly prepared in accordance with the manufacturer's instructions), at room temperature for 30 min. This condition represents a cross-linker to protein ratio of 2:1. The reaction was quenched with 1 M Tris-HCl (pH 7.4). An aliquot of the cross-linked protein was analyzed by SDS-PAGE according to Laemmli (24), and the spots corresponding to monomeric and dimeric species were excised from the gel, washed in 50 mM ammonium bicarbonate, pH 8.0, in 50% acetonitrile, reduced with 10 mM dithiothreitol at 56 °C for 45 min, and alkylated with 55 mM iodoacetamide for 30 min at room temperature in the dark. The gel pieces were washed several times with the buffer, resuspended in 50 mM ammonium bicarbonate, and incubated with 200 ng of endoprotease AspN (ROCHE) overnight at 37 °C. The supernatant containing peptides was analyzed by MALDI-TOF mass spectrometry in reflection mode. Mass calibration was performed using a peptide standard mixture provided by the manufacturer. Subsequently the peptide mixtures obtained by endoprotease AspN digestion were submitted to hydrolysis with 200 ng of trypsin (Sigma) and analyzed by MALDI-TOF mass spectrometry.

## RESULTS

To test the effect of heparin on the aggregation of $\beta_2$-m under pathophysiological conditions, we incubated $\beta_2$-m at 37 °C and pH 6.4 in the presence of type I fibrillar collagen and heparin. The aggregation process was investigated as a function of the incubation time by tapping mode atomic force microscopy. In a previous study (4) we demonstrated that $\beta_2$-m fibrillation under these conditions is strictly localized and associated with the presence of the collagen surface. In the absence of collagen, aggregation experiments performed in the presence of heparin did not give rise to fibril formation. By contrast, in the presence of collagen and heparin, the formation of thin filaments around 1 nm in diameter was observed already after 17-h incubation (Fig. 1*a*), whereas after 24 h fibrils were formed. Fig. 1*b* shows a network of fibrils connecting two isolated collagen fibers, which can easily be recognized due to the characteristic-banding pattern of collagen. A third collagen fibril, shorter and thinner than the other ones and also surrounded by $\beta_2$-m fibrils, is visible in the upper left part of the image; non-fibrillar aggregates are also present. At 48 h fibrils were arranged into planar bundles (Fig. 2*a*). By contrast, under the same conditions but in the absence of heparin, fibrils were still absent, as shown in Fig. 2*b*, which displayed a typical pattern obtained in this case. Several collagen fibers of different diameters are visible; the banding pattern is hidden by the presence of proteinaceous material completely surrounding collagen. The inset shows a magnification of the protein material in the background of Fig. 2*b*, which does not exhibit yet any fibrillar arrangement, whereas annular protofibrils are occasionally observed.

At longer incubation times, the size and morphology of $\beta_2$-m fibrils obtained in the presence of heparin did not change significantly (Fig. 2*c*), suggesting that the aggregation process was complete. Fig. 2*c* shows the typical close-packed arrangement of fibrils in planar sheets, as observed previously for *ex vivo* $\beta_2$-m amyloid fibrils purified from patients affected by dialysis-related amyloidosis (4). Fibrils originated from collagen fibers, which clearly exhibited their banding pattern. Clumps of non-fibrillar material were also present in this sample. In the absence of heparin, fibrils were observed after 4 days incubation (Fig. 2*d*, *inset*), whereas larger fibril bundles were found after 9 days (*d*). The heights of fibrils obtained in the presence and in the absence of heparin were $2.3 \pm 0.4$ and $2.0 \pm 0.4$ nm, respectively. Within the experimental error, these values are compatible and are in agreement with those measured for *ex vivo* $\beta_2$-m amyloid fibrils (4, 25).

A closer inspection of the early stages of the aggregation process in the presence of collagen and heparin is reported in Fig. 3. At the start of the aggregation, globular material was observed (Fig. 3*a*). These globules had a height of $0.80 \pm 0.03$ nm and an apparent width of $32 \pm 1$ nm (the latter is influenced by the

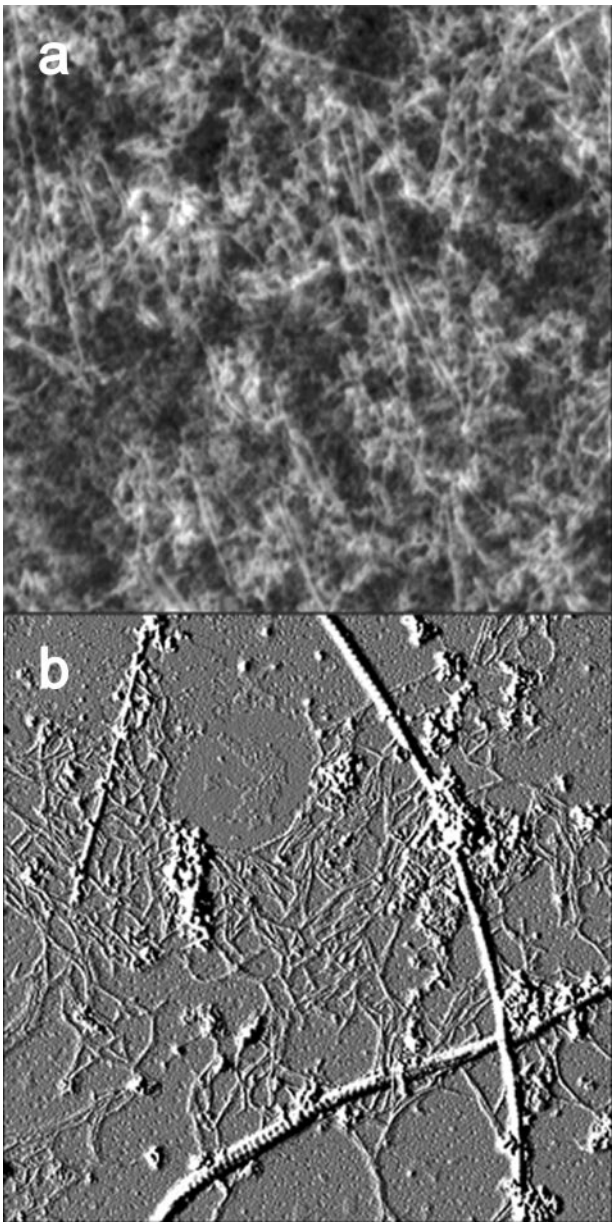


FIGURE 1. **Tapping-mode-AFM images of $\beta_2$-m incubated at 37 °C and pH 6.4 in the presence of fibrillar collagen and heparin.** *a*, after 17 h of incubation thin filaments are clearly visible on a background of non-fibrillar material. Height data: scan size, 1.2 $\mu$m; Z range, 8.0 nm; *b*, fibril network connecting isolated collagen fibrils, observed after 24 h of incubation. Non-fibrillar aggregates are also present. Amplitude data: scan size, 5.7 $\mu$m.

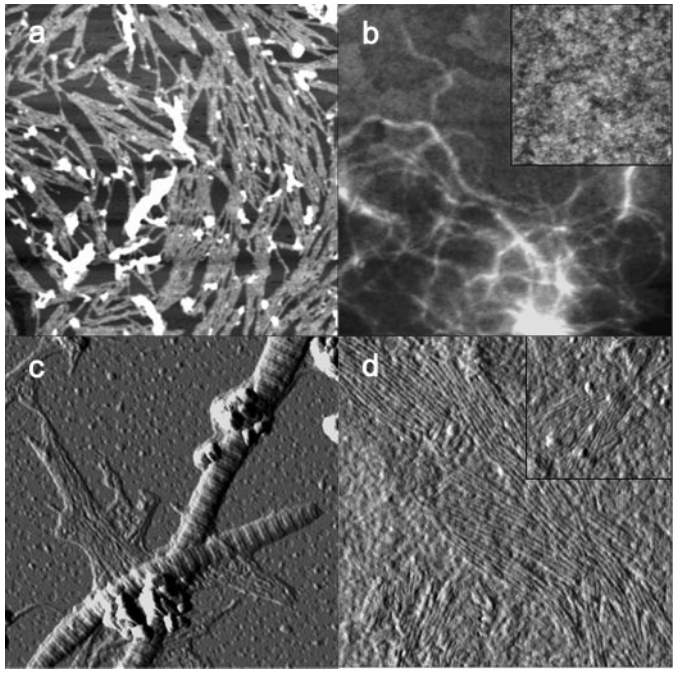


FIGURE 2. **Tapping-mode-AFM images of $\beta_2$-m incubated at 37 °C and pH 6. 4 in the presence of fibrillar collagen (*a* and *c*, with 9 $\mu$M heparin; *b* and *d*, without heparin) (see under "Results").** Incubation time (*a* and *b*, 48 h; *c*, 5 days; *d*, 9 days); *a* and *b*, height data; *c* and *d*, amplitude data. Scan size: *a*, 2.5 $\mu$m; *b*, 3.0 $\mu$m (*inset*, 2.6 $\mu$m); *c*, 1.7 $\mu$m; *d*, 0.84 $\mu$m (*inset*, 0.50 $\mu$m); Z range: *a*, 15 nm, *b*, (*inset*), 10 nm.

tip size). After 2 h this material appeared in part organized into small clusters (Fig. 3*b*); a statistical analysis of the aggregate sizes yielded a height of 0.95 ± 0.05 nm and an apparent width of 40 ± 2 nm. After 4 h short protofibrils, in some cases organized into rings, were observed (Fig. 3*c*). The protofibril height was 0.93 ± 0.02 nm, whereas the length was 92 ± 3 nm. The sample texture observed after 4 h resembles that in the background of Fig. 1*a*, corresponding to 17 h of aggregation, although in the latter a much larger number of rings are visible and longer, straight filaments are also present. For an easier comparison, a portion of Fig. 1*a* is reported in Fig. 3*d* at the same scale of Fig. 3, *a*–*c*.

Although collagen fibers were not always visible in the images presented here, all images were obtained by engaging the AFM tip in close proximity to the collagen network. The filament and fibril sizes reported above were obtained from the height in cross-section of the topographic AFM images; these sizes were reduced with respect to fully hydrated conditions due to the drying procedure applied to the sample to facilitate its adhesion to the mica substrate. A correction factor of about 1.4 was determined based on measurements of the height of globular proteins under full hydration conditions and after drying using a nitrogen stream.[3]

We have previously reported that in similar conditions, but without heparin, the thioflavin assay of $\beta_2$-m was negative. We have now confirmed the previous data, but in the presence of heparin, thioflavin positive aggregates become detectable in solution (Fig. 4). According to the thioflavin assay the fibrillar conversion of full-length $\beta_2$-m is further accelerated by the presence of $\Delta$N6$\beta_2$-m at a concentration that *per se* and within this time course scale does not generate any thioflavin positive aggregate.

To test whether the presence of collagen and heparin might affect the arrangement of the polypeptide chain in $\beta_2$-m fibrils, we employed limited proteolysis, which is an excellent tool to detect the presence of different polypeptide conformations and states of association. Using this technique others and we have shown that the first strand of $\beta_2$-m becomes flexible and susceptible to proteases when the protein is in the fibrillar state (26, 27). In addition, we have shown that trypsin can specifically cleave fibrillar $\beta_2$-m at the peptide bond between Lys-6 and Ile-7, and this bond is fully protected when $\beta_2$-m is in the globular state (26).

[3] S. Giannini, G. Calloni, S. Campioni, X. Salvatella, C. Lagen, S. Gliozzi, A. Relini, M. Vendruscolo, C. M. Dobson, and F. Chiti, submitted for publication.

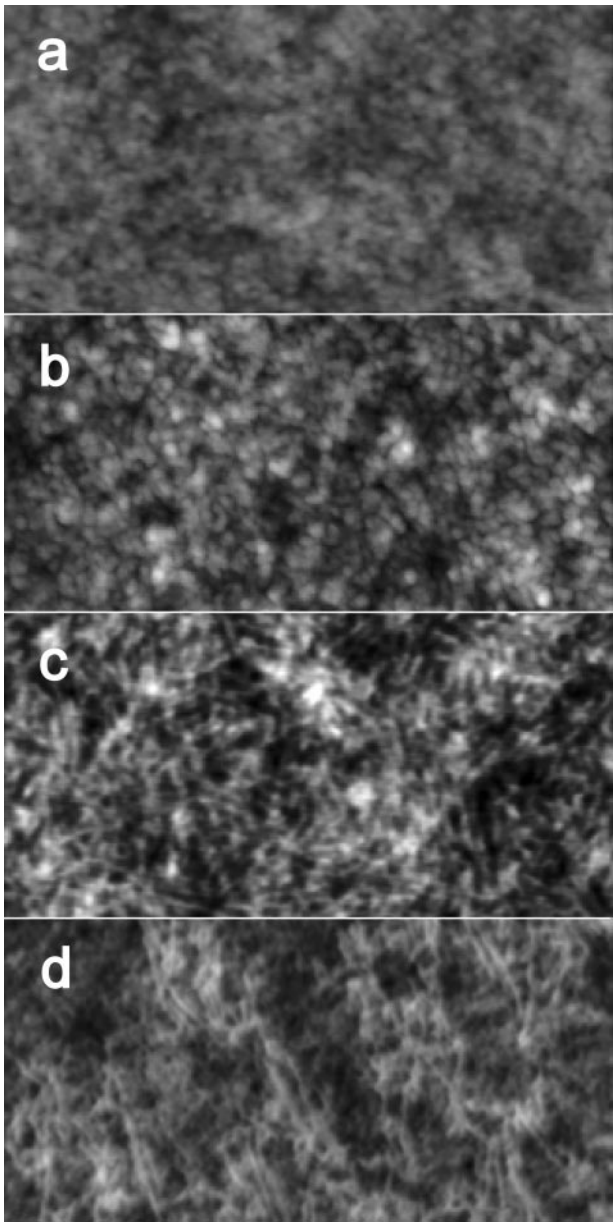


FIGURE 3. **Tapping-mode-AFM images of $\beta_2$-m incubated at 37 °C and pH 6. 4 in the presence of fibrillar collagen and 2 $\mu$M heparin.** *a*, $t = 0$; *b*, after 2 h; *c*, after 4 h; *d*, after 17 h. Each panel corresponds to an image area of 800 nm × 400 nm. Z range, 7 nm.

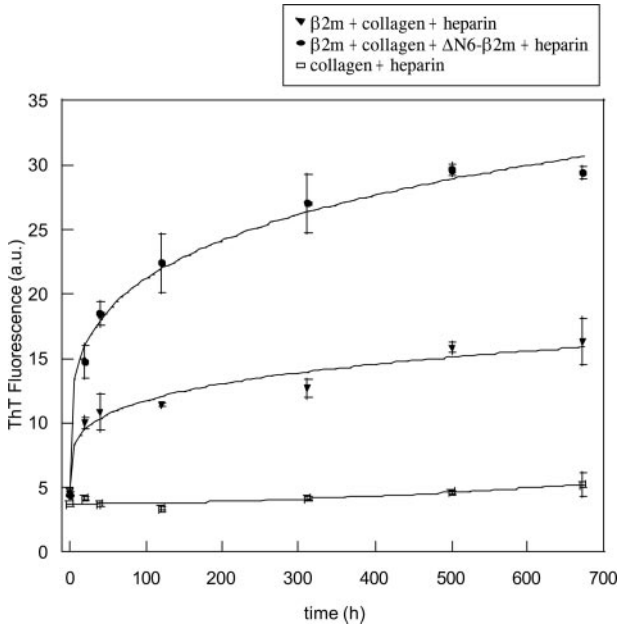


FIGURE 4. **Thioflavin assay of $\beta_2$-m incubated in 50 mM glycine, pH 8.5 at 37 °C.** ▼, samples containing 2 mg/ml $\beta_2$-m, 20 $\mu$g of collagen, and 100 $\mu$g/ml heparin; ●, samples containing 2 mg/ml $\beta_2$-m, 20 $\mu$g of collagen, 100 $\mu$g/ml heparin, and 1 mg/ml $\Delta$N6$\beta_2$-m; □, buffer containing 20 $\mu$g of collagen and 100 $\mu$g/ml heparin.

We have now obtained similar results by monitoring the proteolytic susceptibility of amyloid fibrils grown on collagen in the presence of heparin by using two different enzymes (trypsin and endoprotease AspN). The products obtained exposing the complex collagen-amyloid fibrils to these proteases are substantially identical to those resulting from fibrils formed *in vitro* at low pH. As an example, the cleavage patterns obtained with trypsin on globular $\beta_2$-m, on fibrils of $\beta_2$-m formed *in vitro* at pH 4.0 and fibrils grown on collagen in the presence of heparin are reported in Fig. 5. It is worth noting that all the cleavage sites described in the past (20, 26) were confirmed with fibrils prepared under the present conditions, thus suggesting that the general topology of the protein inside the fibrils is similar, independently from the method of *in vitro* fibrillogenesis that is used. Apparently the presence of collagen does not mask the sensitive sites of cleavage of fibrillar $\beta_2$-m. This clue is consistent with the AFM images, which show that contact between collagen and amyloid fibrils is at most limited to one fibril edge. In fact, $\beta_2$-m fibrils grown in very close proximity to collagen fibers lie almost perpendicular to the latter (see Figs. 1*b* and 2*c*), as expected for a growth process influenced by the radial electric field of the collagen fiber (4).

The strong effect of heparin on fibril growth raises a seminal question about the mechanism by which this highly charged polyanion might accelerate the fibril formation. We previously reported that the presence of soluble $\beta_2$-m oligomers (removable by filtration with 20-nm pore filters) was also capable of speeding up the kinetic of fibrillogenesis in the presence of collagen (4). Therefore, heparin might act on this process favoring the formation of oligomers; we have tested this hypothesis by light scattering measurements of $\beta_2$-m in solution. This set of experiments was necessarily performed in the absence of fibrillar collagen because the large size of the collagen network interfered with light scattering measurements. However, we demonstrated previously that the presence of collagen is a crucial factor to achieve the fibrillation of wild type $\beta_2$-m at 37 °C and pH 6.4 (4). Therefore, light scattering experiments were not expected to reproduce in detail the morphologies found in the presence of collagen, but rather to yield information about the ability of heparin to accelerate the aggregation process. $\beta_2$-m was filtered with a 20-nm pore filter and was incubated at 37 °C and pH 6.4 in acetate buffer in the presence of heparin. Fig. 6 shows the dynamic light scattering correlation functions measured in the absence and in the presence of heparin at pH 6.4 at different incubation times in a typical experiment. The curves obtained in the presence of heparin clearly show a change in the decay rate, which increases as the $\beta_2$-m aggregation time

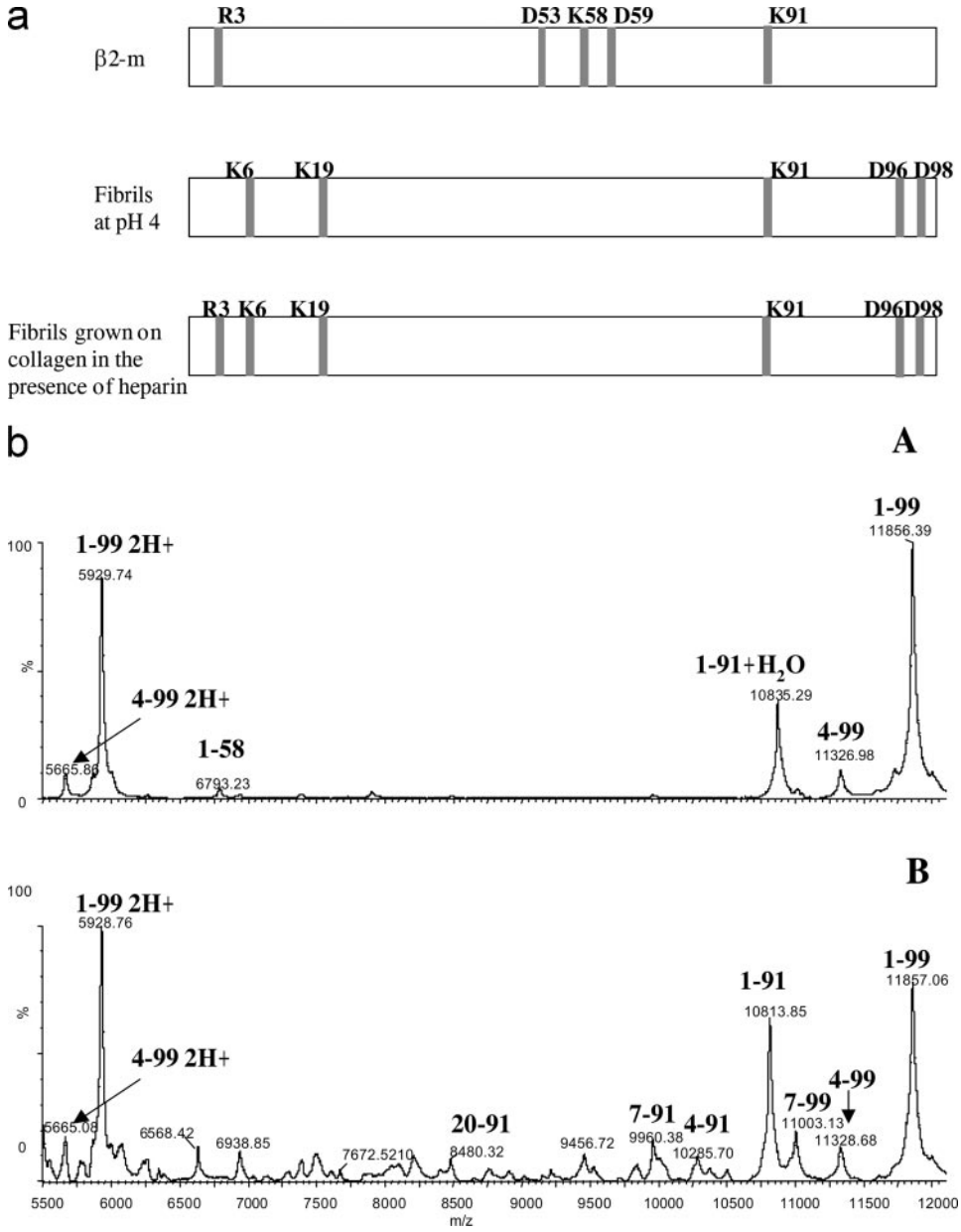


FIGURE 5. *a*, schematic representation of the results obtained from limited proteolysis experiments on the soluble form of native $\beta_2$-m and on fibrils formed *in vitro*. Preferential cleavage sites are depicted by *solid bars*. Trypsin and endoprotease AspN were used as conformational probes. *b*, MALDI/mass spectrometry analysis (only spectra in the range 5500–12000 are shown) of the aliquots withdrawn following 1 h of trypsin incubation of the soluble $\beta_2$-m (*A*) and the fibrils grown in the presence of collagen and heparin (*B*).

increases. On the other hand, the decay rate of the curves obtained in the absence of heparin does not change significantly with $\beta_2$-m aggregation time. In the absence of heparin and at short aggregation times in the presence of heparin, a fast decay of the correlation function is observed. A qualitative analysis of the correlation functions using the algorithm implemented in our instrument indicated the presence of particles with size in the range of 2–6 nm, which may correspond to monomeric $\beta_2$-m and oligomers of few molecules. At longer aggregation times in the presence of heparin, the decay rate of the correlation function was much slower. In this case the analysis of the correlation functions showed the coexistence of small and large particles, from a few nanometers to hundreds of nanometers.

The same experiment was also performed in parallel at pH 7.4. In this case a fast decay of the correlation function was always observed in the presence of heparin, without significant differences with respect to the sample in the absence of heparin. In both cases the correlation functions showed the same behavior even after 6 days incubation at 37 °C (not shown). In the absence of heparin we did not observe the growth of aggregates of typical size (hundreds nm), reported to occur after 4 days at pH 7.4 and 25 °C in a previous study (28). This result is probably due to the lower $\beta_2$-m concentration employed in the present work. The AFM results, supported by the light scattering results reported here, suggest that heparin can accelerate the fibrillogenesis in the presence of collagen by favoring $\beta_2$-m aggregation. Even the minimal concentration of heparin (0.6 $\mu$M) that we tested was able to activate aggregation. It is worth noting that such a concentration can be easily achieved during the hemodialysis procedure according to the doses of heparin infused to avoid blood clotting (29).

The presence of oligomers in solution has been further explored by trying to stabilize their intermolecular interactions through chemical cross-linkers able to covalently bridge the side chains of the lysines. We have chosen to cross-link lysines because from the tertiary structure of the monomer (Protein Data Bank code 1JNJ) the 8 lysines of $\beta_2$-m are regularly distributed on the molecular surface and well exposed to the solvent (Fig. 7). Through this approach it is possible to stabilize multimers of $\beta_2$-m that can be visualized and singled out through the SDS-PAGE. By electrophoresis we can actually well separate multimers from monomers to hexamers and identify the side chains involved in the intermolecular cross-linkages (Fig. 8*A*). When the cross-linker is not present (Fig. 8, *lane a*), the oligomers are solubilized, but in the presence of cross-linkers, $\beta_2$-m in solution gives rise to several discrete bands (*lane b*). The proteolytic digestion of the isolated bands gives rise to a peptide fingerprint in which free lysines, lysines interconnected through intramolecular links, and those involved in intermolecular links can be easily isolated. Fig. 8*B* shows two comparative spectra of the peptide fingerprints derived from monomeric

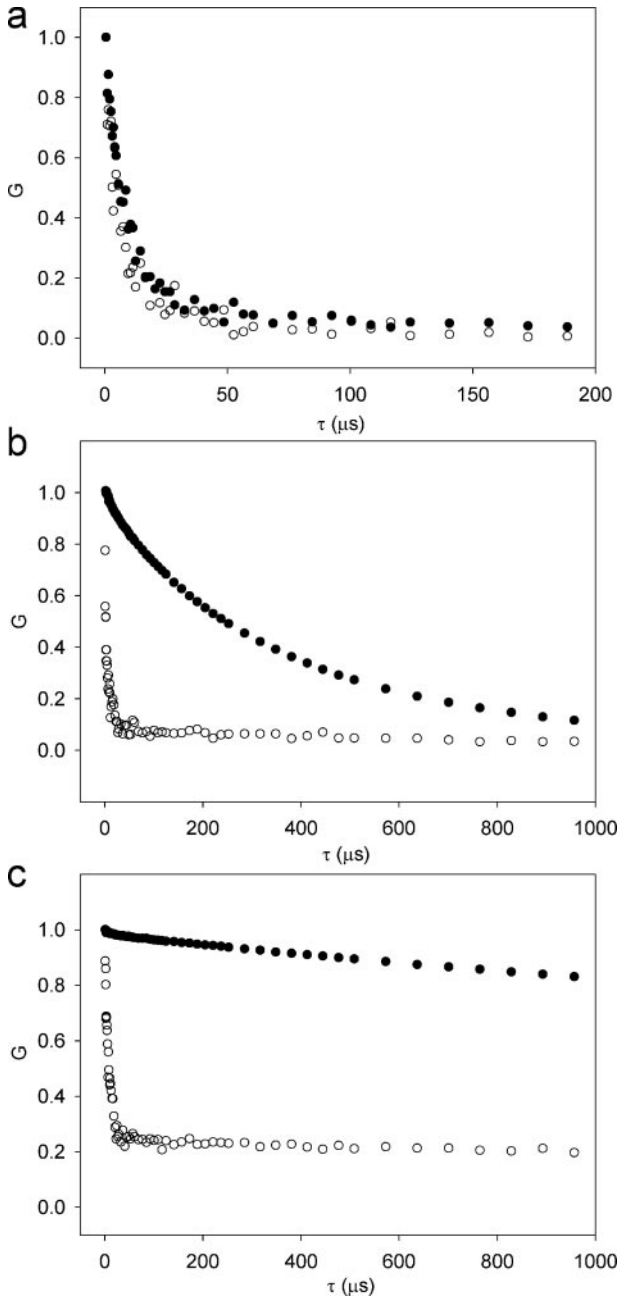


FIGURE 6. **Dynamic light scattering auto-correlation function G($\tau$) measured for $\beta_2$-m solutions kept at 37°C and pH 6.4 (*a*, 2 h; *b*, 24 h; *c*, 5 days) in the absence (*empty circles*) and in the presence (*filled circles*) of 2 $\mu$M heparin.**

and dimeric bands excised from the SDS-PAGE. A peptide of 3236 dalton, that is not present in the monomeric band, can be isolated in dimers after digestion with AspN protease. This peptide can only correspond to an intermolecular peptide connecting Lys-58 and Lys-91 or Lys-94. It is well established that when the $NH_2$ group of lysine is involved in the amide bond with the cross-linker, the trypsin cleavage does not occur. Therefore to identify which one of the two C-terminal lysines is involved in the cross-linkage, we have sub-digested, by trypsin, the peptides obtained from the endoprotease AspN cleavage. We always obtained from this digestion a peptide of 2255 dalton in which the Lys-91 escapes from cleavage, thus demonstrating that its side chain is directly involved

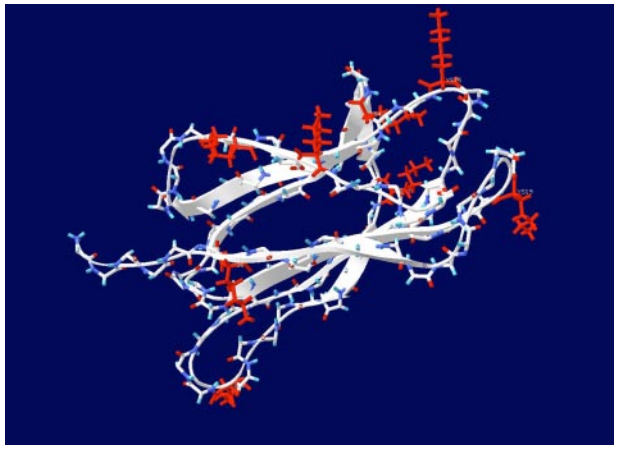

FIGURE 7. **Three-dimensional structure of monomeric $\beta_2$-m (Protein Data Bank code 1JNJ) in which the side chains of eight lysines of the protein are highlighted in *red*.**

in the linkage. We exclude that this cross-linked dipeptide might originate from a single molecule because the minimal linear distance of the $\epsilon$-amino group of Lys-58 from those of Lys-91 and- 94 is, respectively, of 30 and 36 Å, a distance that could be never covered by the cross-linker of 7 Å that we have used. This is the only intermolecular peptide found in dimers, trimers, tetramers, pentamers, and hexamers. We are unable, at this stage, to provide any structural detail regarding the limits of the contact area between the monomeric units. However, these data and preliminary data obtained with other chemical cross-linkers suggest that in the oligomers the loop DE of $\beta_2$-m might be involved preferentially into interactions with surface regions of the protein extended from the N-terminal site of strand G and the N-terminal site of strand A.

The same type of cross-linking identified in the $\beta_2$-m dimer is confirmed in trimers, tetramers, and pentamers. It is worth noting that this type of interaction is present both in the presence and in the absence of heparin (data not shown), thus suggesting that at least in the early phase of oligomerization, heparin only enhances the intrinsic propensity of $\beta_2$-m to self-assemble through specific intermolecular interactions.

## DISCUSSION

It is commonly accepted that amyloid fibril formation results from a nucleation and growth process and that the presence of a lag phase reflects the time required for nuclei to form (30). We found that upon filtration with 20-nm pore size filters, to maximize the removal of possible pre-existing seeds, $\beta_2$-m solutions incubated at 37 °C and pH 6.4 in the presence of collagen and heparin-produced fibrils within 1 day from the start of the aggregation process. Under the same conditions, but in the absence of heparin 4 days were required to obtain fibrils. Light scattering measurements showed that heparin favors $\beta_2$-m aggregation, as after 1 day aggregates of hundreds nm were formed, whereas in the absence of heparin only oligomeric forms were detected even after 5 days of aggregation. These measurements, being performed in the absence of collagen, were not expected to reproduce the same aggregation path observed in the presence of collagen, but they provided complementary information about the ability of heparin to accelerate the aggregation

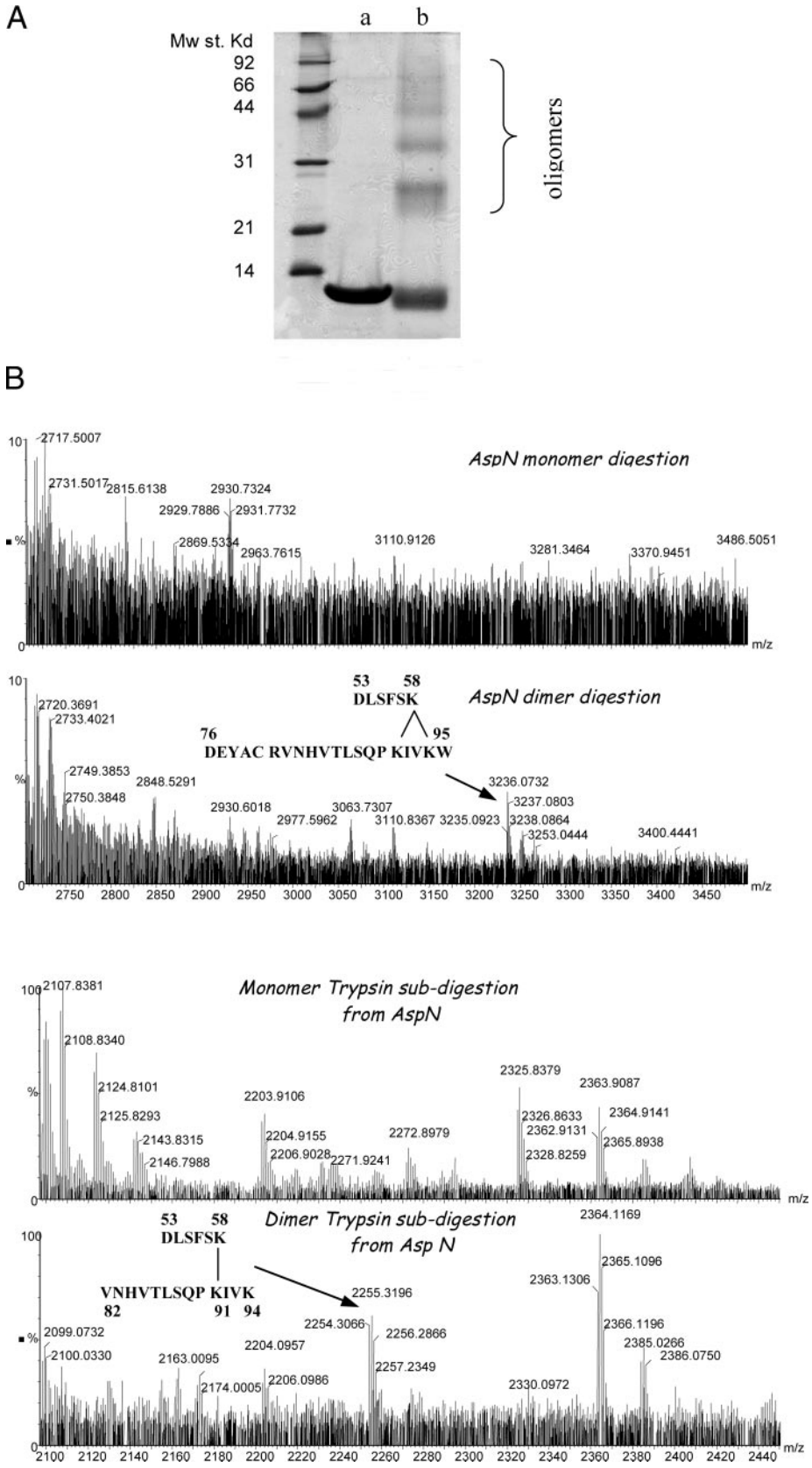


FIGURE 8. **Analyses of covalently stabilized $\beta_2$-m oligomers obtained by chemical cross-linking.** *A*, SDS-PAGE of soluble (*lane a*) and cross-linked $\beta_2$-m (*lane b*). *B*, the *first two panels* show the MALDI-TOF analyses of the endoprotease AspN digest of monomeric and dimeric $\beta_2$-m, respectively. The *last two panels* show the mass spectra of peptide fingerprints obtained after trypsin sub-digestion of endoprotease AspN peptides mixture of monomeric and dimeric $\beta_2$-m. The *arrow* indicates the mass of the intermolecular peptide connecting Lys-58 and Lys-91 isolated in $\beta_2$-m oligomers.

process. Collectively, the AFM and light scattering results suggest that heparin may favor the $\beta_2$-m oligomerization and consequently the fibrillogenesis in a manner similar to what occurs in other amyloid-forming proteins such as gelsolin (11). At the pH investigated in this work, $\beta_2$-m has a net negative charge, as confirmed by the negative value of the $\zeta$ potential ($-10 \pm 5$ mV) measured in these conditions (4). It is surprising that a polyanion such as heparin could favor the aggregation process; however, a similar behavior has been already observed for negatively charged $\alpha$-synuclein (10). It has been suggested that in this case either the presence of clusters of positive charges or the dipolar nature of the global charge distribution may be involved in the interaction with heparin. In addition, the binding of heparin has been proposed to increase the degree of order of the protein, thus favoring the aggregation process (31).

The ability of heparin to stabilize and favor the formation of oligomers, even though the affinity measured between heparin and monomeric $\beta_2$-m is very low (32), suggests that oligomeric species might be the preferential target of heparin. The remarkable differences in the kinetics of oligomerization observed at pH 6.4 or 7.4, in the absence of any significant conformational change in the protein at these two pHs, as observed in the past by NMR (33, 34), confirm previous suggestions (35) that His residues might have an important role in the oligomerization and interaction with heparin. In fact, these are the only residues that could change their ionization state between pH 6.4 and 7.4. The stabilization of the oligomers through chemical cross-linkers suggests that at least in the smallest oligomers an interaction head to tail of the molecule is present in the early phase of the aggregation.

The combination of collagen fibers and heparin seems so far the most potent amyloid inducer under

pathophysiological conditions for full-length $\beta_2$-m, and it might represent a model for further investigation of both inhibitors and positive effectors of polymerization. This model might also represent a system for the evaluation of events, such as proteolysis, that could remodel, stabilize, or dissolve amyloid fibrils. We have clearly established that in natural amyloid fibrils, the full-length protein is the predominant species, but a form lacking the first six N-terminal residues ($\Delta N6\beta_2$-m) also exists (25, 36). The remarkable amyloidogenic propensity of this species, in comparison with the full-length protein, and its ability to form fibrils at neutral pH is well documented (20, 27).

In this study we have shown that $\Delta N6\beta_2$-m can be generated from full-length $\beta_2$-m aggregated over the collagen surface; it is therefore plausible that *in vivo* $\Delta N6\beta_2$-m might be formed at the site of deposition of $\beta_2$-m on collagen through the action of a putative protease. $\Delta N6\beta_2$-m, once formed, could certainly contribute to the acceleration of the process of amyloid deposition, being capable of recruiting the full-length protein in the oligomerization process (28). It has been recently shown that heparin and heparan sulfate, even without seeds, can induce the fibrillogenesis of $\Delta N6\beta_2$-m in physiological buffer, thus further supporting the hypothesis that the concomitant presence of $\Delta N6\beta_2$-m and glycosaminoglycans highly enhances the risk of amyloid formation (19). Deposition on collagen is favored when $\beta_2$-m is oligomeric (4) as well as when it is cleaved as $\Delta N6\beta_2$-m (3). All our data, so far, envisage a model of "nucleation dependent" fibrillogenesis funneled toward the collagen surface. We have previously reported a low affinity interaction ($K_d \cong 100$ $\mu$M) between monomeric full-length $\beta_2$-m and collagen (3), but it has been established that oligomerization thermodynamically favors the interaction of a ligand with its target surface (37) and therefore oligomeric $\beta_2$-m could represent the species most avidly binding the collagen surface.

*Acknowledgments—We thank Claudio Canale for help with the AFM measurements. We also thank Piero Pucci, Maria Monti, and Gennaro Esposito for continuous critical discussion on this subject.*

## REFERENCES


1. Porcelli, S. A., and Modlin, R. L. (1999) *Annu. Rev. Immunol.* **17,** 297–329
2. Homma, N. (1989) *Nephron* **53,** 37–40
3. Giorgetti, S., Rossi, A., Mangione, P., Raimondi, S., Marini, S., Stoppini, M., Corazza, A., Viglino, P., Esposito, G., Cetta, G., Merlini, G., and Bellotti, V. (2005) *Protein Sci.* **14,** 696–702
4. Relini, A., Canale, C., De Stefano, S., Rolandi, R., Giorgetti, S., Stoppini, M., Rossi, A., Fogolari, F., Corazza, A,. Esposito, G., Gliozzi, A., and Bellotti, V. (2006) *J. Biol. Chem.* **281,** 16521–16529
5. Kielty, C. M., Hopkinson, I., and Grant, M. E. (1993) *Connective Tissue and its Heritable Disorders* (Royce P. M. and Steinmann B., eds) pp. 103–147, Wiley-Liss Inc., New York
6. Miyata, T., Nakano, T., Masuzawa, M., Katsuoka, K., and Kamata, K. (2005) *J. Dermatol.* **32,** 410–412
7. Lindahl, U. (2007) *Thromb. Haemost.* **98,** 109–115
8. McLaurin, J., Franklin, T., Zhang, X., Deng, J., and Fraser, P. E. (1999) *Eur. J. Biochem.* **266,** 1101–1110
9. Castillo, G. M., Lukito, W., Wight T. N., and Snow, A. D. (1999) *J. Neurochem.* **72,** 1681–1687
10. Cohlberg, J. A., Li, J., Uversky, V. N., and Fink, A. L. (2002) *Biochemistry* **41,** 1502–1511
11. Suk, J. Y., Zhang, F., Balch, W. E., Linhardt, R. J., and Kelly, J. W. (2006) *Biochemistry* **45,** 2234–2242
12. Yamamoto, S., Yamaguchi, I., Hasegawa, K., Tsutsumi, Goto, Y., Gejyo F., and Naiki, H. (2004) *J. Am. Soc. Nephrol.* **15,** 126–133
13. Snow, A. D., and Kisilevsky, R. (1985) *Lab. Investig.* **53,** 37–44
14. Li, J. P., Galvis, M. L., Gong, F., Zhang, X., Zcharia, E., Metzger, S., Vlodavsky, I., Kisilevsky, R., and Lindahl, U. (2005) *Proc. Natl. Acad. Sci. U. S. A.* **102,** 6473–6477
15. Kisilevsky, R., Lemieux, L. J., Fraser, P. E., Kong, X., Hultin, P. G., and Szarek, W. A. (1995) *Nat. Med.* **1,** 143–148
16. Ikizler, T. A., and Schulman, G. (2005) *Am. J. Kidney Dis.* **46,** 976–981
17. Yamaguchi, I., Suda, H., Tsuzuike, N., Seto, K., Seki, M., Yamaguchi, Y., Hasegawa, K., Takahashi, N., Yamamoto, S., Gejyo, F., and Naiki, H. (2003) *Kidney Int.* **64,** 1080–1088
18. Myers, S. L., Jones, S., Jahn, T. R., Morten, I. J., Tennent, G. A., Hewitt, E. W., and Radford, S. E. (2006) *Biochemistry* **45,** 2311–2321
19. Borysik, A. J., Morten, I. J., Radford, S. E., and Hewitt, E. W. (2007) *Kidney Int.* **72,** 174–181
20. Esposito, G., Michelutti, R., Verdone, G., Viglino, P., Hernandez, H., Robinson, C. V., Amoresano, A., Dal Piaz, F., Monti, M., Pucci, P., Mangione, P., Stoppini, M., Merlini, G., Ferri, G., and Bellotti, V. (2000) *Protein Sci.* **9,** 831–845
21. Huszar, G., Maiocco, J., and Naftolin, F. (1980) *Anal. Biochem.* **105,** 424–442
22. LeVine, H. (1993) *Protein Sci.* **2,** 404–410
23. Khlebtsov, N. G. (2003) *Colloid J.* **65,** 652–655
24. Laemmli, K. (1970) *Nature* **227,** 680–685
25. Giorgetti, S., Stoppini, M., Tennent, G. A., Relini, A., Marchese, L., Raimondi, S., Monti, M., Marini, S., Ostergaard, O., Heegaard, N. H., Pucci, P., Esposito, G., Merlini, G., and Bellotti, V. (2007) *Protein Sci.* **16,** 343–349
26. Monti, M., Principe, S., Giorgetti, S., Mangione, P., Merlini, G., Clark, A., Bellotti, V., Amoresano, A., and Pucci, P. (2002) *Protein Sci.* **11,** 2362–2369
27. Myers, S. L., Thomson, N. H., Radford, S. E., and Ashcroft, A. E. (2006) *Rapid Commun. Mass Spectrom.* **20,** 1628–1636
28. Piazza, R., Pierno, M., Iacopini, S., Mangione, P., Esposito, G., and Bellotti, V. (2006) *Eur. Biophys. J.* **35,** 439–445
29. Fareed, J., Hoppensteadt, D., Schultz, C., Ma, Q., Kujawski, M. F., Neville, B., and Messmore, H. (2004) *Curr. Pharm. Des.* **10,** 983–999
30. Chiti, F., and Dobson, C. M. (2006) *Annu. Rev. Biochem.* **75,** 333–366
31. Calamai, M., Kumita, J. R., Misfud, J., Parrini, C., Ramazzotti, M., Ramponi, G., Taddei, N., Chiti, F., and Dobson, C. M. (2006) *Biochemistry* **45,** 12806–12815
32. Ohashi, K., Kisilevsky, R., and Yanagishita, M. (2002) *Nephron* **90,** 158–168
33. Verdone, G., Corazza, A., Viglino, P., Pettirossi, F., Giorgetti, S., Mangione, P., Andreola, A., Stoppini, M., Bellotti, V., and Esposito, G. (2002) *Protein Sci.* **11,** 487–499
34. Okon, M., Bray, P., and Vucelic, D. (1992) *Biochemistry* **31,** 8906–8915
35. Ancsin, J. B. (2003) *Amyloid* **10,** 67–79
36. Bellotti, V., Stoppini, M., Mangione, P., Sunde, M., Robinson, C., Asti, L., Brancaccio, D., and Ferri, G. (1998) *Eur. J. Biochem.* **258,** 61–67
37. Minton, A. P. (1995) *Biophys. J.* **68,** 1311–1322

# Heparin Strongly Enhances the Formation of $\beta_2$-Microglobulin Amyloid Fibrils in the Presence of Type I Collagen

Annalisa Relini, Silvia De Stefano, Silvia Torrassa, Ornella Cavalleri, Ranieri Rolandi, Alessandra Gliozzi, Sofia Giorgetti, Sara Raimondi, Loredana Marchese, Laura Verga, Antonio Rossi, Monica Stoppini and Vittorio Bellotti

*J. Biol. Chem. 2008, 283:4912-4920.*
*doi: 10.1074/jbc.M702712200 originally published online December 3, 2007*

---